

Influence of Cobalt on the Structure and Properties of Micro-arc Oxidation Coatings on 2A12 Aluminum Alloys

Liqin Shen

School of Rail Transportation, Nanjing Vocational Institute of Transport Technology, Nanjing, China

Abstract:

A blue ceramic coating was applied on 2A12 aluminium alloy by microarc oxidation (MAO) in the presence of CoSO_4 . The morphology, phase constituent, corrosion resistance and wear resistance of 2A12 aluminium alloy microarc oxidation coatings were characterized by various techniques. The MAO coatings were found to be smoother and denser when CoSO_4 was used to the electrolyte. Also, In terms of corrosion resistance and wear resistance, the microarc oxidation coating prepared by CoSO_4 is superior to that without CoSO_4 .

Keywords: *Microarc oxidation, CoSO_4 , Wear resistance, Corrosion resistance.*

I. INTRODUCTION

Microarc oxidation has received a lot of attention due to its effectiveness and convenience in preparing thick oxide ceramic coatings on alloys such as Al, Ti, Mg and their alloys. Also known as plasma electrolytic oxidation (PEO). The coating formed by micro-arc oxidation process generally has high hardness. It also has a good metallurgical bonding with the substrate. At the same time, the oxide film shows excellent corrosion resistance and wear resistance [1, 2]. Moreover, because this process is conducted with the use of liquids, coating more complexly shaped materials is efficient [3, 4].

Some researchers have sought to even further improve the properties of MAO coatings. Enhanced corrosion resistance has been achieved with the addition of additives [5-7]. Shi et al. [8] found that the solution with EDTA resulted in better corrosion resistance which made coatings thinner and uniform. When $\text{Na}_2\text{B}_4\text{O}_7$ is added to the solution, the pitting corrosion resistance performance of the coating is improved which made coatings thicker and compact. Additionally, Tang et al. [9] found that the addition of $\text{Co}(\text{CH}_3\text{COO})_2$ to the electrolyte enhanced the emissivity of the coating.

To study the effect of CoSO_4 , CoSO_4 was added to a silicate electrolyte system in this study. MAO coatings were deposited onto a 2A12 aluminium alloy. The microstructure, phase structure, corrosion and wear resistance of the microarc oxidation coatings were studied in depth formed in experimental silicate electrolyte system with and without CoSO_4 .

II. EXPERIMENTAL

To be tested specimens (25 mm × 20 mm × 4 mm) of the 2A12 aluminium alloy (3.9-5.0 Cu, 1.2-1.8 Mg, 0.3-0.9 Mn, Al balanced, mass fraction, %) were used in MAO experiments. Before MAO treatment, the sample surface is polished manually, from large to small according to the particle size of sandpaper, until it is polished with 20 micron SiC polishing paste. After washing with deionized water, it is blowed dry with a hair dryer. The MAO electrolyte consists of sodium silicate at a concentration of 10g/l, sodium hydroxide at 2.0 g/l and sodium fluoride at 0.8 g/l and CoSO₄ at 1.2 g/l. The contrast concentration does not contain CoSO₄. In the experiment, a 30 kW pulse power supply was self-made. MAO process was carried out in water -cooled electrolytic cell. The the alloy served as the anode, while the stainless-steel electrolyte was the cathode. During MAO treatment, the cathodic voltage was kept at 80V and the anodic voltage at 460V. The positive and negative duty ratios were 45%, and the positive and negative frequencies were 300 and 150 Hz, respectively. The duration time was 40 min. In order to obtain better experimental results, the temperature of treatment was always kept at 10±2°C by a recyclable water cooling system. The surface morphologies of MAO coatings were observed with JSM-6380LV. Phase structure was verified by an XD-3A X-ray diffractometer with the following settings: Cu K α radiation, $\lambda=1.5804$ and a scan speed of 5o/min. The coefficient of friction of the coatings was measured on a MFT-3000 (Rtec) under a load of 26 N for 30 min, and the counterpart was a GCr15 steel ball (4 mm in diameter, HRC63-65). Electrochemical measurements were tested by the Parstat 2273 electrochemical workstation. A platinum sheet (20 mm×20 mm square slice) is used as the counter electrode and a saturated calomel electrode (short for SCE) as the reference electrode. The experimental environment was with the solution was naturally aerated and an exposed area of 1cm², NaCl solution with concentration of 3.5% at room temperature. By a scanning rate of 5 mV/s, Potentiodynamic polarization curves were acquired.

III. RESULTS AND DISCUSSION

The surface morphologies of a MAO coating formed is significantly different from that of the electrolyte with and without CoSO₄, as shown in Fig. 1. The surface of the film presents a crater like porous morphology. Cracks were also observed on the surface of the film. Under the action of e, molten oxides were formed on the alloy surface with the applied voltage in reported. Under the violent cooling of electrolyte solution, huge thermal stress was generated to crack the film, as shown in Fig. 1a-b. Large molten oxide particles and island structures were distributed at random on the coating surface produced without CoSO₄ (Fig. 1a). The MAO coating formed in the electrolyte with CoSO₄ had smaller molten oxide particles and pancake-like structures (Fig. 1b). When CoSO₄ was added to the electrolyte, the surface of the film was flat and smooth. The roughness was 4.6 microns, and the void diameter in the film was small. However, when there was no CoSO₄ in the electrolyte, the surface of the film was rough, the roughness was 12.5 microns, and the surface density was low. This may be due to the addition of soluble CoSO₄ in the electrolyte and the adsorption of cationic CO²⁺ on the alloy surface, which provided more nucleation sites for the formation of the film and was conducive to the formation of dense and smooth film.

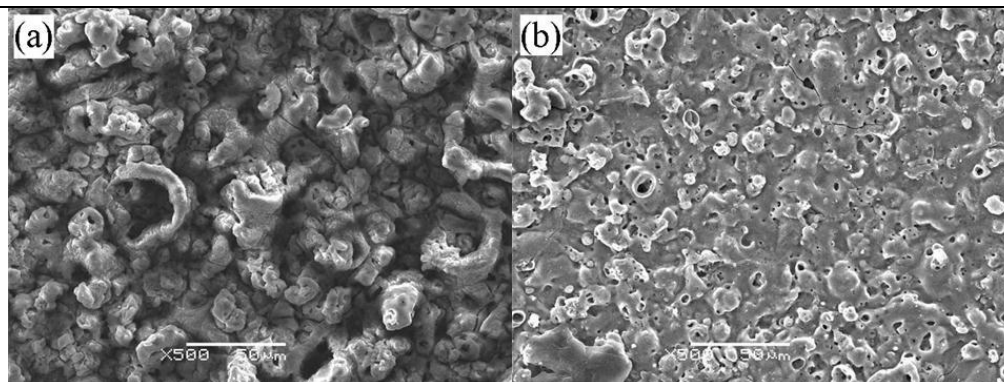


Fig 1 Surface morphology of MAO coatings in electrolyte without additive CoSO₄ (a) and with CoSO₄ (b)

The X-ray diffraction patterns of the MAO coatings formed in the electrolyte with and without CoSO₄ additive as well as that of the uncoated 2A12 alloy are shown in Fig. 2. It is found that the MAO coating is mainly composed of α -Al₂O₃ and γ -Al₂O₃ phases, regardless of CoSO₄ or no CoSO₄ in the electrolyte.

The highest peak in the X-ray diagram is the peak of Al, which corresponded to the aluminum alloy substrate and were found since the X-rays penetrated through the coating. By comparison, we found that the coating formed with CoSO₄ resulted in a decreased intensity of the XRD peak in the Fig.2 for Al, which indicates that the film thickness is increased and dense. Although some Co was detected on the MAO coating surface by EDS, peaks of crystal phases were not found to be associated with cobalt oxides due to their low contents.

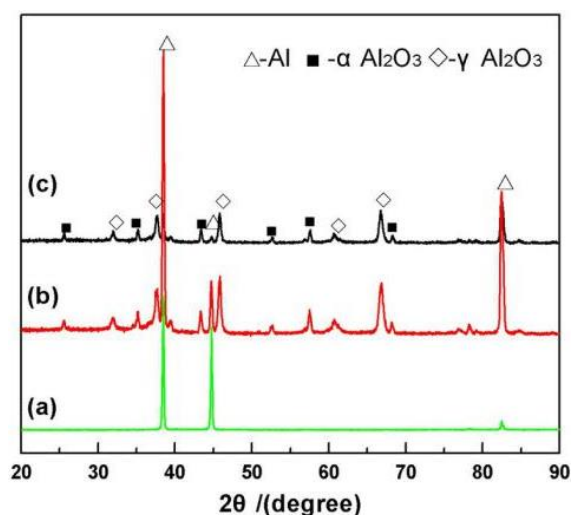


Fig 2 XRD patterns of samples: (a) substrate; (b) without CoSO₄; (c) with CoSO₄

The polarization curves of the MAO coatings formed in the different electrolytes are shown in Fig. 3. The values of corrosion current density (i_{corr}) and corrosion potential (E_{corr}) were extrapolated from the polarization curve, and the results are summarized in Table 1. When CoSO₄ is added to the electrolyte, the anodic polarization curve and current density curve of the film increase slowly with the increase of applied voltage. When there is no CoSO₄ in the electrolyte, the anodic current density curve of the film increases rapidly with the increase of applied voltage. The coating formed with CoSO₄ had a higher anodic branch

slope than without CoSO₄. This is due to the presence of CoSO₄ in the electrolyte, the internal micro defects (such as microcracks) of the formed film are few, the diameter of the surface oxidation hole is small, and a dense film is formed as a barrier layer, which effectively hinders the invasion of Cl⁻ ions in the corrosion solution and reduces the corrosion rate. This indicates that the coating formed in CoSO₄ electrolyte solution has fewer microdefects and a more compact structure, which is beneficial to inhibit Cl⁻ transfer in the corrosion process. The self-corrosion potential E_{corr} reflects the trend of easy corrosion of materials. The more positive the self-corrosion potential, the less likely the corrosion will occur. The self corrosion current density reflects the corrosion rate of materials. The greater the self corrosion current density is, the greater the corrosion reaction rate is. The self-corrosion current density of the film formed by adding CoSO₄ to the electrolyte is the smallest, which is 5.349, which is 3 orders of magnitude lower than that of the base aluminum alloy and 1 order of magnitude lower than that without CoSO₄ in the electrolyte. It has excellent corrosion resistance.

The corrosion potential (E_{corr}) and corrosion current density (i_{corr}) are important parameters for evaluating how well the coatings can protect the alloy from corrosion. A higher corrosion potential and a lower i_{corr} indicated that the coating had a better corrosion resistance.

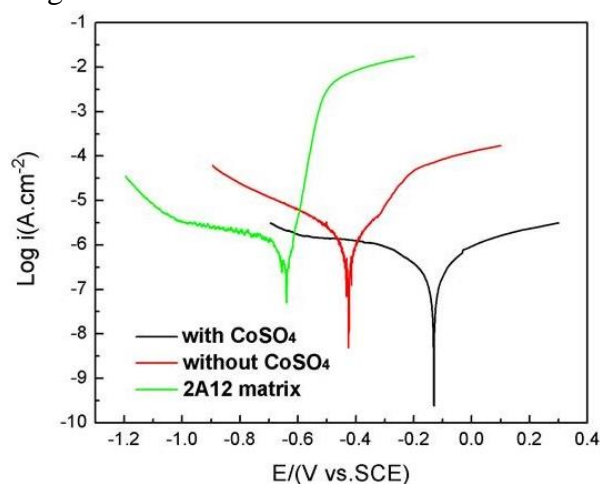


Fig 3 Tafel curves of matrix (a), MAO coatings in electrolyte without additive CoSO₄ (b) and with CoSO₄ (c)

TABLE. I Extrapolation results of the polarization curves of the coatings prepared with and without CoSO₄ in the electrolyte

Sample	$E_{Corr}(mV)$	$I_{corr}(A.cm^2)$
2A12 matrix	-719.652	2.240×10^{-6}
Without CoSO ₄	-271.798	6.691×10^{-8}
With CoSO ₄	-128.543	5.349×10^{-9}

Fig. 4 shows the friction coefficient varied with respect to the sliding time. The friction coefficient of the matrix and the MAO coating followed distinctly different trends with varying sliding time. The matrix resulted in a sharp peak at the beginning of the test, which increased to a higher value with increasing sliding time but then decreased. Also for the matrix, the friction coefficient gradually increased after

sliding for about 100 s, and the final friction coefficient was about 0.8. The friction coefficient of the MAO coatings formed in the different electrolytes exhibited an opposite trend than that of the matrix. The friction coefficient of the MAO coatings decreased with increasing sliding time, and the final friction coefficients of the MAO coatings with and without CoSO_4 were about 0.45 and 0.50, respectively. The friction coefficient of the MAO coating formed in electrolyte with CoSO_4 was lower than that of MAO coating formed in electrolyte without CoSO_4 , and this was mainly attributed to the dense and smooth surface.

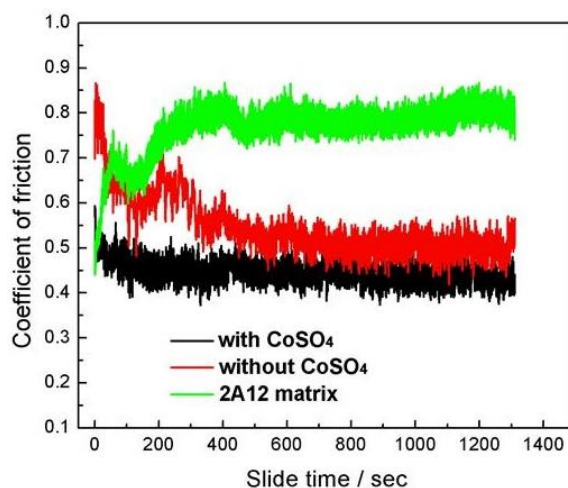


Fig 4 Variation of friction coefficients during reciprocating wear: 2A12 matrix (a), MAO coatings in electrolyte without additive CoSO_4 (b) and with CoSO_4 (c)

IV. CONCLUSION

MAO coatings were obtained in electrolytes with and without CoSO_4 on 2A12 aluminum alloys. When CoSO_4 is added to the electrolyte, the film is dense and smooth. Co element was detected on the surface of the film, but no phase containing Co was detected. The micro arc oxidation film formed when CoSO_4 is added to the electrolyte has low friction coefficient and self corrosion current density, and has better comprehensive properties than the film without CoSO_4 .

The MAO coating formed exhibited better abrasive and corrosion resistances in the electrolyte with CoSO_4 than without CoSO_4 .

ACKNOWLEDGEMENTS

This research was supported by High Research Project for Teacher Professional Leaders of Higher Vocational Colleges in Jiangsu (Grant No. 2020GRFX055) and Transportation Vocational Education and Scientific Research Project in the National Transportation Vocational Education and Teaching Steering Committee (Grant No. 2019A02).

REFERENCES

- [1] Guo HX, Liu ZY, Wang YX, Li JL (2021). Tribological mechanism of micro-arc oxidation coatings prepared by different electrolyte systems in artificial seawater. *Ceramics International*, 47(6):7344-7352.
- [2] Wang WZ, Feng SS, Li ZM, Chen ZG, Zhao TY (2020). Microstructure and properties of micro-arc oxidation ceramic films on AerMet100 steel. *Journal of Materials Research and Technology*, 9(3):6014-6027.
- [3] Zhao QZ, Li W, Mei QZ, Rong CZ, M. Bobby Kannan, Cun GL, Yu FZ (2020). Biodegradation behavior of micro-arc oxidation coating on magnesium alloy-from a protein perspective. *Bioactive Materials*, 5(2):398-409
- [4] Sinebryukhov SL, Gnedenkova AS, Mashatlyar DV, Gnedenkova SV (2010). PEO-coating/substrate interface investigation by localised electrochemical impedance spectroscopy. *Surf Coat Technol*, 205:1697-1701.
- [5] Ekbal Mohammed Saeed, Nawal Mohammed Dawood, Sahar Falah Hasan (2021). Improvement corrosion resistance of Ni-Ti alloy by TiO₂ coating and hydroxyapatite/TiO₂ composite coating using micro arc oxidation process. *Materials Today: Proceedings*, 2:2789-2796
- [6] Tawfik Hamood Qaid, S.Ramesh, F.Yusof, Wan Jeffrey Basirun, Y.C.Ching, Hari Chandran, S.Ramesh, S.Krishnasamy (2019). Micro-arc oxidation of bioceramic coatings containing eggshell-derived hydroxyapatite on titanium substrate. *Ceramics International*, 45: 18371-18381.
- [7] Chen QZ, Li WZ, Ling K, Yang RX (2020). Effect of Na₂WO₄ addition on formation mechanism and microstructure of micro-arc oxidation coating on Al-Ti double-layer composite plate. *Materials & Design*, 190,108558.
- [8] Shi LL, Xu YJ, Li K, Yao ZP, Wu SQ. Effect of additives on structure and corrosion resistance of ceramic coatings on Mg-Li alloy by micro-arc oxidation. *Curr Appl Phys*, 10 (2010):719-723.
- [9] Tang H, Sun Q, Xin TZ, Yi CG, Jiang ZH, Wang FP (2012). Influence of Co(CH₃COO)₂ concentration on thermal emissivity of coatings formed on titanium alloy by micro-arc oxidation. *Curr Appl Phys*, 12:284-290.